Lasers in Manufacturing Conference 2025

Transparent polycarbonate welding: exploring the effects of scanning speed and fluence per pulse on weld seam quality

Soheil Alee Mazreshadi[a], Pol Vanwersch[a,b], Tim Evens[b], Sylvie Castagne[a]

[a]KU Leuven, Department of Mechanical Engineering and Flanders Make@KU Leuven-M&A, Celestijnenlaan 300, 3001 Leuven, Belgium
[b]KU Leuven, Department of Materials Engineering, Diepenbeek Campus, Wetenschapspark 27, 3590 Diepenbeek, Belgium

Abstract

Laser welding is a precise material joining technique offering localized heating and a minimal heat-affected zone. For transparent polymers without an absorber layer, ultrafast pulses can trigger non-linear phenomena needed for welding. This study optimizes the scanning speed and fluence per pulse for welding polycarbonate using a 1.03 µm wavelength femtosecond laser. The cumulative fluence is calculated at the weld seam center and edge to determine the maximum and minimum energy per unit area, and the weld seam quality is assessed optically. Optimal results are achieved at scanning speeds of 10 and 20 mm/s with fluence per pulse of 0.38 – 0.72 J/cm^2 and 0.65 – 1.14 J/cm^2, respectively. Two damage regimes are identified: one caused by high cumulative fluence at low speeds (5 mm/s), and the other by high fluence per pulse (1.50 J/cm^2) at high speeds (30 mm/s). These findings reveal how energy deposition shapes weld seam morphology and quality.

Keywords: femtosecond lasers; laser welding; non-linear absorption; transparent polymers; polycarbonate

1. Introduction

The bonding of polymers is gaining attention because of its ability to produce complex, multi-material assemblies that are highly valued in advanced micromanufacturing industries such as electronics, automotive, and healthcare (Friedrich & Almajid, 2013; Osellame et al., 2011; Wan et al., 2020). However, conventional bonding techniques—such as adhesive bonding, thermal welding, mechanical fastening, etc.—often fail to meet the requirements of high-precision manufacturing. These methods are frequently limited by issues such as biocompatibility concerns, poor dimensional control and extensive post-processing steps, making them less suitable for micro-scale systems (Temiz et al., 2015; Volpe et al., 2021; Zhang et al., 2017). In microfluidic systems and similar domains, the quality of the weld seam is critical: imperfections or inconsistencies at the seam can compromise structural integrity, introduce leakage, or impair device performance (Temiz et al., 2015; Tsao & DeVoe, 2009). Ultrashort pulsed (USP) laser welding offers high spatial precision, making it particularly advantageous for delicate or microstructured substrates. USP's defining characteristics—extremely short pulse durations and high peak intensities—enable nonlinear absorption phenomena. When tightly focused on the interface of two transparent polymer substrates, ultrafast laser pulses induce nonlinear absorption, resulting in localized heating, softening, and partial melting of the polymer. Upon rapid cooling, polymer chains from both substrates may interdiffuse across the interface, forming a permanent weld.

Despite significant progress in laser-based bonding of similar and dissimilar materials—such as glass-glass, glass-metal, glass-semiconductor, and metal-polymer systems—the application of ultrashort pulsed (USP) lasers to weld transparent polymers remains relatively underexplored (Bardin et al., 2007; Kim et al., 2018; Mingareev et al., 2012; Schricker et al., 2020; Xu et al., 2023). The findings of Volpe et al. show that successful bonding of PMMA substrates using femtosecond laser pulses, achieving microfluidic channels capable of withstanding internal pressures up to 1 bar (Volpe et al., 2015). The study by Roth

et al. indicates that higher scanning speeds are possible while maintaining good bond strength for the COC polymer when pulse overlap and focal positioning are carefully optimized (Roth et al., 2016a). More recently, Capodacqua et al. reports successful bonding of PMMA to silicon, highlighting the importance of interfacial absorption and thermal expansion mismatch in achieving reliable adhesion across dissimilar materials (Capodacqua et al., 2023). While these studies contribute valuable insights into process feasibility and mechanical performance, they often overlook weld seam quality, including its geometry, uniformity, and defect formation. Additionally, the spatial distribution of fluence—particularly at the center versus the edges of the weld—remains insufficiently characterized. These aspects are critical for understanding the laser–polymer interaction mechanisms and for improving the repeatability and visual quality of the weld seam in precision applications.

This study focuses on the morphological quality of the weld seam produced by a Gaussian beam in multiphoton polymer welding, as the weld seam plays a critical role in defining the material fusion zone and directly impacts the reliability and integrity of the joint. Specifically, it investigates how fluence per pulse and scanning speed influence the formation of a homogeneous weld seam. These parameters are systematically varied to calculate the cumulative fluence and analyze its spatial distribution across the weld line. At higher energy regimes, partial absorption of the Gaussian beam occurs before the focal plane, leading to an axial offset between the intended and actual weld locations. This offset increases with energy and must be considered in fluence calculations. To account for this, the axial position (z) is defined based on the measured offset, and the radial distance(r) is taken as half the measured seam width. These coordinates are then used to calculate the cumulative fluence at the center and edges of the weld seam, enabling identification of a process window where stable, defect-free welding can be achieved. While mechanical strength is not assessed in this work, its significance is acknowledged and will be addressed in future studies.

2. Materials and methodology

2.1. Experimental setup and characterization

The thermoplastic material used is 1.5 mm-thick polycarbonate (PC) plates (PyraSied). PC has high stiffness (Young's modulus: 2.35 GPa), transparency, and low shrinkage, making it a well-suited option for point-of-care devices application, such as microneedle components and cancer-on-a-chip systems (Liu et al., 2025; Vanwersch et al., 2024). All samples are cut into plates with dimensions 75 mm × 15 mm × 1.5 mm. Although the polymer is supplied with a protective cover, it is cleaned with ethanol before processing. The spectral properties of polycarbonate (PC) are analyzed using a UV–VIS–NIR spectrometer (Agilent Cary 60 UV-VIS) to verify its transparency at the laser wavelength of 1030 nm.

The optomechanical system consists of a 20 W femtosecond laser source (Carbide, Light Conversion), a beam delivery path, a 2-axis optical galvanometer scanner, and an associated electronic control unit. Experiments are conducted at 18°C. The laser has a wavelength of 1030 ± 10 nm, a Gaussian beam profile with linear polarization, and an M^2 factor of <1.2. The maximum repetition rate is 1 MHz, with a pulse duration of 250 fs and a beam waist of 15 μm (radius at $1/e^2$).

The experimental setup for bonding transparent polymers using an ultrashort pulsed laser is illustrated in Figure 1a. The laser beam is directed through a galvo scanner and focused by an F-theta lens with a focal length of 125 mm into the interface between two transparent polymer plates mounted on an XY-stage. As shown in Figure 1b, the plates are pressed together using a pneumatic clamping system (Festo EV-20/75), which applies a maximum force of 600 N under 0.6 MPa air pressure to ensure intimate contact during laser processing. Although the laser light is focused at the interface, nonlinear absorption can occur earlier within the top plate if the incoming laser pulses have sufficient intensity to exceed the threshold for multiphoton absorption. This results in a vertical offset between the focal point and the actual weld seam. This absorption behavior is shown schematically in Figure 2a, where the absorbed area shifts upward due to the Gaussian intensity profile of the focused beam. A camera aligned along the laser axis is used to measure this offset and monitor the location of the processed area relative to the initial focus. After each experiment and before disassembling the setup, weld lines are inspected using an in-system camera positioned along the beam axis. A telecentric lens (Edmund Optics, #21823; 8× magnification, 65 mm working distance) is used to measure the position of the weld seam top relative to the interface, allowing identification of the vertical offset (z). An adjustment of the focal plane position is demonstrated by Roth et al. to be necessary under varying welding speeds to achieve effective bonding—an observation that is further supported by the offset correction approach adopted in this work (Roth et al., 2016b). To evaluate the lateral weld quality, a digital microscope (Keyence VHX-6000) is employed to image the weld seam top view and measure the radial width (r) across the bonded interface, as illustrated in Figure 2b.

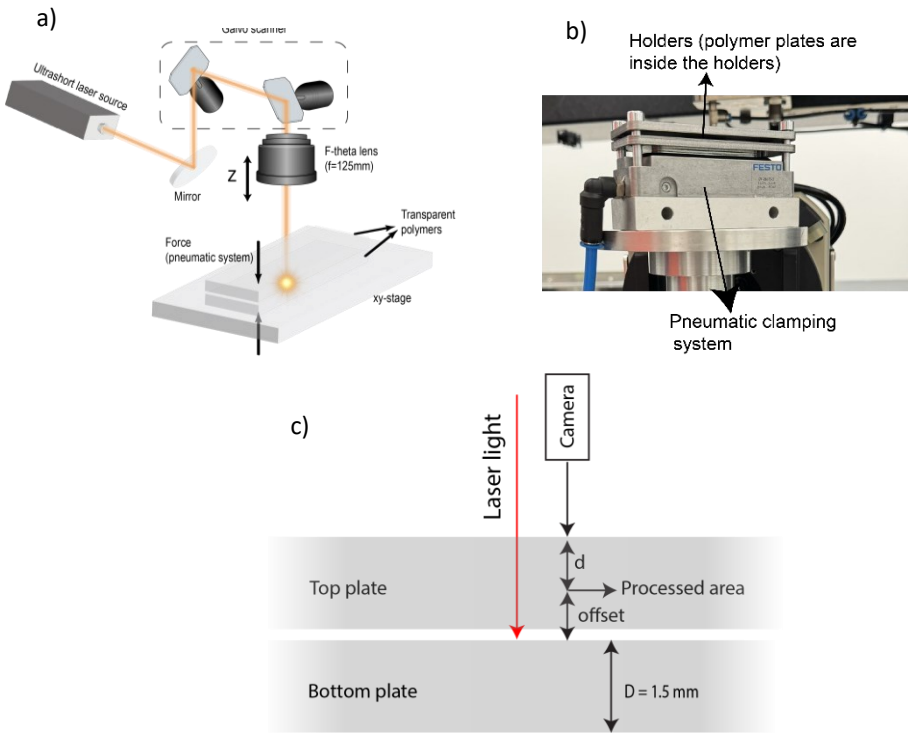

Figure 1. a) schematic overview of the laser setup, b) photo of the pneumatic clamping system and c) laser focus and weld seam offset in transparent polymer bonding

2.2. Theoretical calculations

Cumulative fluence (F_{Cum}) is crucial to understanding the bonding mechanism of transparent polymers, as it reflects the effects of multiple pulses instead of focusing solely on individual pulse fluence. The heat accumulation, structural changes,

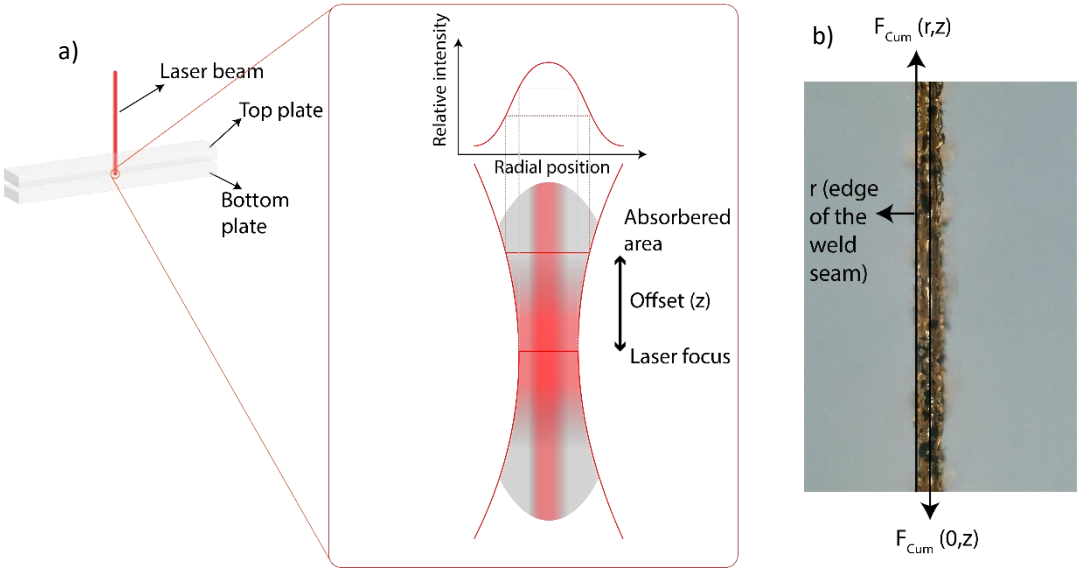

Figure 2. a) Schematic representation of light absorption by the polycarbonate (cross-section) and b) weld seam top view

and chemical reactions in the material depend on the total energy delivered over time, not just the energy from a single pulse. Thus, the cumulative fluence of the weld seam is calculated at both the center and the edges as they reflect the processed area with maximum and minimum delivered energy areas, respectively (considering the Gaussian profile). Figure 2 shows the schematic of light absorption in polycarbonate and the top view of the weld seam. The offset (z) is measured using the telecentric camera, and the weld width is obtained from top-view microscopy. For a Gaussian beam, the cumulative fluence can be calculated using the fluence $F(r,z)$ at a radial distance r from the beam axis and at position z and the effective number of pulses per unit area as follows (Fox & Mücklich, 2023):

$$F_{Cum}(r,z) = F(r,z) \times n_{eff} \quad (1)$$

$$F(r,z) = F_0 \left(\frac{\omega_0}{\omega(z)}\right)^2 \exp\left(-2\frac{r^2}{\omega(z)^2}\right) \quad (2)$$

$$F_0 = \frac{2E}{\pi\omega_0^2} \quad (3)$$

$$\omega(z) = \omega_0\sqrt{1+\left(\frac{z}{z_R}\right)^2} \quad (4)$$

$$z_R = \frac{\pi\omega_0^2}{\lambda} \quad (5)$$

where F_0 is the peak fluence at the focus ($z = 0$), ω_0 is the beam waist, $\omega(z)$ is the beam radius at distance z, E *is the pulse energy,* Z_R is Rayleigh's range and λ is the laser source wavelength.

n_{eff} is the effective number of pulses per unit area, defined as:

$$n_{eff} = \frac{1}{1-OL} \quad (6)$$

where OL is the pulse overlap, defined as:

$$OL = \frac{2\times r^2 \times cos^{-1}\left(\frac{\Delta x}{2r}\right) - \frac{\Delta x}{r}\times\sqrt{4\times r^2\times\Delta x^2}}{\pi \times r^2} \quad (7)$$

where Δx is the distance between consecutive pulses.

3. Results and discussion

Figure 3 shows the UV-Vis-near IR spectroscopy results, indicating that the polycarbonate used is nearly 90 percent transparent at the laser working wavelength of 1030 nm. The absorption spectrum reveals that the material begins to absorb light in the UV range around 390 nm, corresponding to a bandgap of 3.18 eV. Given the photon energy of the laser at 1.203 eV, at least 3 photons are required to excite the electrons of polycarbonate from relaxed to excited states. The high transparency of polycarbonate allows for working within the volume of the material, enabling intricate micromachining processes. This characteristic implies that the underlying mechanism must be non-linear to effectively trigger the desired processes.

To evaluate the energy distribution within the bonded region, the cumulative fluence is calculated at both the center and the edges of the weld seams. The total amount of energy per unit area can be calculated by applying z (measured using the

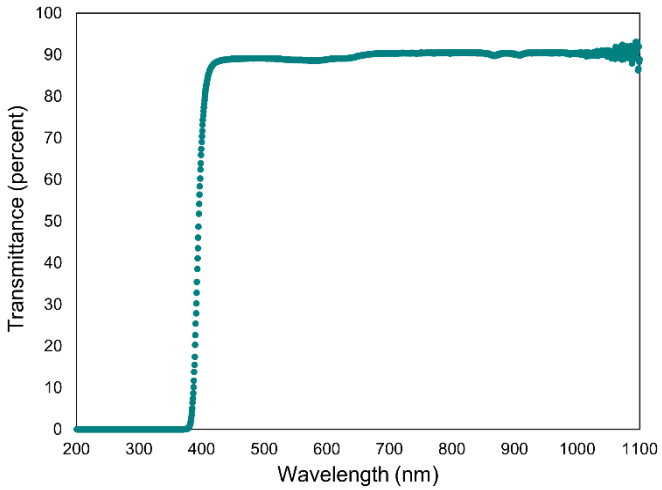

Figure 3. Transmittance spectrum from UV-Vis-Near IR spectroscopy of polycarbonate.

system's internal camera) and r (half of the width of the weld seam) into equation 1. The fluence at two key points—the

edges and the center of the weld— is of particular interest. The center value represents the maximum fluence delivered to the area, as the radial distance (r) is zero, whereas the minimum energy is delivered to the edges. Line-writing experiments, in which fluence per pulse and scanning speeds are varied, are conducted to identify the optimal parameters for producing uniform, defect-free weld seams. The fluence per pulse ranges from 0.08 to 1.78 J/cm^2 and scanning speeds of 5, 10, 20 and 30 mm/s are studied. Although wider ranges of fluence per pulse and scanning speeds are initially investigated, values that caused noticeable optical damage or failed to result in bonding are excluded from further analysis.

Figure 4 illustrates the cumulative fluence at the center and edge of the weld seam, corresponding to locations receiving maximum and minimum energy, respectively. The relationship between cumulative fluence $F_{Cum}(0,z)$ (J/cm^2), and fluence per pulse (J/cm^2) at different scanning speeds are shown in Figure 4a.

The cumulative fluence at the seam center increases steadily with the fluence per pulse for each scanning speed. Because scanning speed influences the effective pulse overlap, it directly affects the cumulative fluence; lower scanning speeds result in higher pulse overlap and thus higher cumulative fluence. Consequently, combinations of low scanning speeds and high fluence per pulse are omitted from this set of experiments due to the risk of material damage caused by excessive heat accumulation and an enlarged heat-affected zone. Under these conditions, extreme values of fluence per pulse should be adjusted to prevent damage to the material.

As shown in Figure 4a, increasing the scanning speed reduces cumulative fluence. This is expected since fewer pulses overlap at higher speeds. As a result, the fluence per pulse must be increased at higher scanning speeds to maintain effective energy deposition for bonding. However, increasing the fluence per pulse beyond a certain threshold can lead to local damage or burning of the polycarbonate due to the excessive intensity of each pulse. For instance, based on experimental

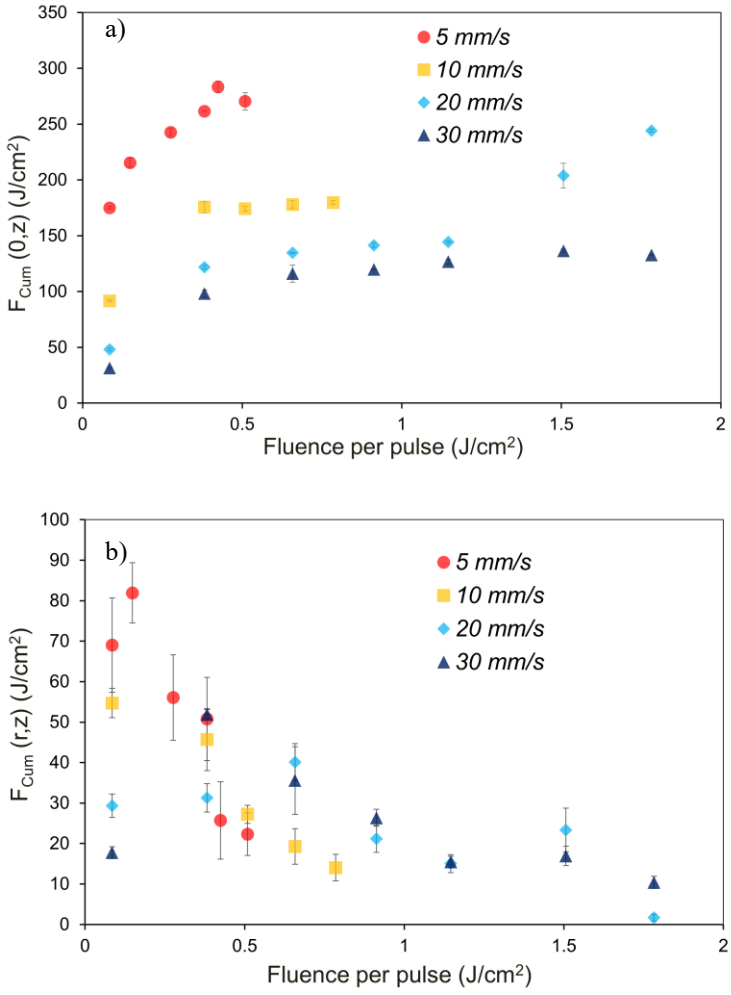

Figure 4. The cumulated fluence of the weld seam: a) at the center, b) at the edge

observations, at a scanning speed of 5 mm/s, the maximum fluence per pulse that can be applied without burning is approximately 0.50 J/cm^2 inducing the cumulative fluence of 531.3 J/cm^2. For higher scanning speeds of 10 mm/s and 20 mm/s, the corresponding maximum cumulative fluences without visible damage are 374.2 J/cm^2 and 496.2 J/cm^2, respectively. These are associated with fluence per pulse values of 0.78 J/cm^2 and 1.78 J/cm^2. At 30 mm/s bonding is still achievable at a fluence per pulse of 1.78 J/cm^2 , resulting in a cumulative fluence of 296.1 J/cm^2. These results suggest that cumulative fluence alone is not a sufficient parameter to predict bonding effectiveness, as it also depends on laser machining parameters. Instead, a balance must be found between fluence per pulse and scanning speed to ensure enough nonlinear absorption occurs for bonding without inducing thermal damage.

Figure 4b illustrate the relationship between cumulative fluence, $F_{Cum}(r,z)$ (J/cm^2), and fluence per pulse (J/cm^2) at various scanning speeds. As expected, the cumulative fluence generally decreases with increasing scanning speed. However, cumulative fluence and fluence per pulse are not directly correlated. At lower fluence per pulse, laser pulses pass through the polymer and concentrate at the focal point, resulting in a smaller beam diameter. This confines the energy distribution to a tighter region, leading to higher energy density at the weld seam, including the edges of the weld seam. In contrast, as the fluence per pulse increases, the incoming light possesses sufficient energy to trigger nonlinear absorption before reaching the nominal focus, depending on the energy level. This causes energy deposition to begin earlier along the beam path, as previously discussed. Considering the Gaussian beam profile, the beam diameter is smallest at the focus and increases with distance away from the focus. Therefore, this premature absorption of light causes the energy to spread over a larger volume, resulting in a broader weld seam. Thus, at lower fluence per pulse levels, the cumulative fluence tends to be higher and more concentrated, which is beneficial for achieving stronger and more predictable bonds. Moreover, while the cumulative fluence at the center of the beam may increase or stabilize with increasing fluence per pulse, the gap between the center and edge fluences also increases. This growing inhomogeneity in energy distribution makes the welding process less uniform and can negatively impact weld quality.

Figure 5 shows the microscopic images of weld seams at various cumulative fluences and speed levels.

As seen in the images in the 5 mm/s column, the weld seams contain black spots, indicating localized burning of the polycarbonate caused by higher cumulative fluence values—an undesirable outcome. In contrast, the weld seams at scanning speeds of 10 mm/s and 20 mm/s show greater homogeneity and fewer black spots. This observation suggests that lower accumulated fluence at higher scanning speeds leads to reduced thermal damage. To ensure effective bonding despite the reduced pulse overlap at high scanning speeds, higher fluence per pulse values are necessary. More specifically, at a scanning speed of 30 mm/s, the fluence per pulse levels are generally high, increasing the risk of burning the polycarbonate, while at lower energy levels, effective bonding does not occur (Nguyen et al., 2018). Therefore, polycarbonate can be damaged either by excessive cumulative fluence at low scanning speeds or by high fluence per pulse at high scanning speeds. Overall, the optimal range for achieving uniform weld seams with minimal thermal damage lies between 10 and 20 mm/s, with corresponding fluence per pulse values of 0.38 – 0.78 J/cm^2 and 0.65 - 1.14 J/cm^2, respectively.

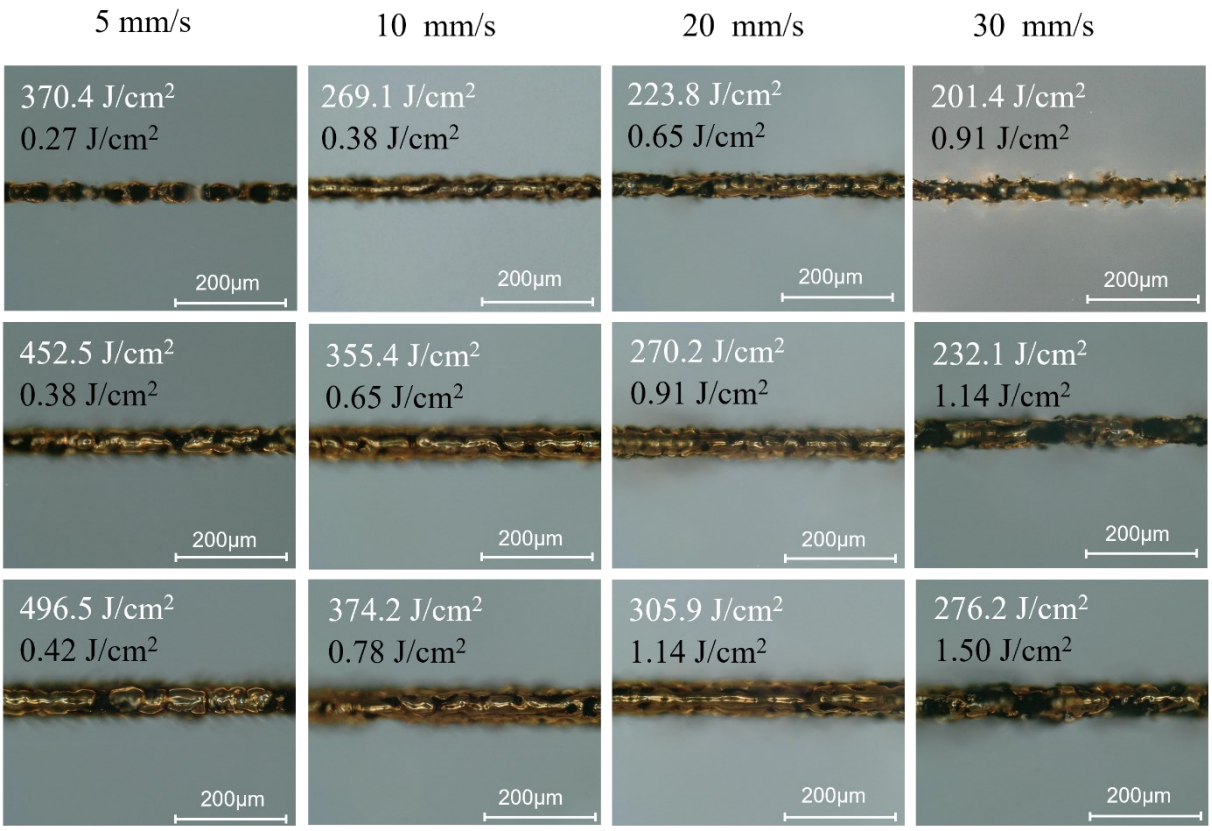

Figure 5. 3D digital images of weld seams at different scanning speeds and pulse energies at 500 kHz. The white font indicates the cumulative fluence, while the black font represents the fluence per pulse.

4. Conclusion

This study explores the influence of scanning speed and fluence per pulse on the weld seam quality of transparent polycarbonate using femtosecond laser pulses. Four scanning speeds—5, 10, 20, and 30 mm/s—are evaluated across a fluence range of 0.06 to 1.78 J/cm^2. The results reveal that excessive energy input can degrade weld quality, either due to high cumulative fluence at lower speeds (e.g., 5 mm/s) or excessive fluence per pulse at higher speeds (e.g., 30 mm/s), both lead to material damage such as burning. Optimal weld seams are achieved at intermediate scanning speeds of 10 and 20 mm/s, indicating that these parameters are critical for achieving high-quality weld seams in polycarbonate. These findings underscore the importance of balancing cumulative fluence and fluence per pulse to optimize the laser micromachining process. Future work should investigate the roles of repetition rate and overscan strategies in enhancing bond strength and weld integrity.

Acknowledgements

This work was funded by the KU Leuven Interdisciplinary Network project Fonds Wetenschappelijk Onderzoek – Vlaanderen (FWO) SBO – S003923N APPLIEDx: Integrated point-of-care platform for infectious diseases diagnosis, as well as the through the FWO Medium-Scale Research Infrastructure project FemtoFac (I001120N) and FWO SB fellowship 1S31022N granted to P.V.

References

Bardin, F., Kloss, S., Wang, C. H., Moore, A. J., Jourdain, A., De Wolf, I., & Hand, D. P. (2007). Laser bonding of glass to silicon using polymer for microsystems packaging. *Journal of Microelectromechanical Systems*, *16*(3), 571–580. https://doi.org/10.1109/JMEMS.2007.896704

Capodacqua, F. M. C., Volpe, A., Gaudiuso, C., & Ancona, A. (2023). Bonding of PMMA to silicon by femtosecond laser pulses. *Scientific Reports*, *13*(1). https://doi.org/10.1038/s41598-023-31969-y

Fox, T., & Mücklich, F. (2023). Development and Validation of a Calculation Routine for the Precise Determination of Pulse Overlap and Accumulated Fluence in Pulsed Laser Surface Treatment. *Advanced Engineering Materials*, *25*(3). https://doi.org/10.1002/adem.202201021

Friedrich, K., & Almajid, A. A. (2013). Manufacturing aspects of advanced polymer composites for automotive applications. *Applied Composite Materials*, *20*(2), 107–128. https://doi.org/10.1007/s10443-012-9258-7

Kim, S., Kim, J., Joung, Y. H., Choi, J., & Koo, C. (2018). Bonding strength of a glass microfluidic device fabricated by femtosecond laser micromachining and direct welding. *Micromachines*, *9*(12). https://doi.org/10.3390/mi9120639

Liu, L., Wang, H., Chen, R., Song, Y., Wei, W., Baek, D., Gillin, M., Kurabayashi, K., & Chen, W. (2025). Cancer-on-a-chip for precision cancer medicine. *Lab on a Chip*. https://doi.org/10.1039/D4LC01043D

Mingareev, I., Weirauch, F., Olowinsky, A., Shah, L., Kadwani, P., & Richardson, M. (2012). Welding of polymers using a 2 µm thulium fiber laser. *Optics and Laser Technology*, *44*(7), 2095–2099. https://doi.org/10.1016/j.optlastec.2012.03.020

Nguyen, N. P., Fatherazi, P., Nippgen, S., Brosda, M., Olowinsky, A., & Gillner, A. (2018). Investigations on energy deposition in polycarbonate by picosecond laser pulses for welding applications. *Procedia CIRP*, *74*, 315–319. https://doi.org/10.1016/j.procir.2018.08.122

Osellame, R., Hoekstra, H. J. W. M., Cerullo, G., & Pollnau, M. (2011). Femtosecond laser microstructuring: An enabling tool for optofluidic lab-on-chips. In *Laser and Photonics Reviews* (Vol. 5, Issue 3, pp. 442–463). https://doi.org/10.1002/lpor.201000031

Roth, G. L., Rung, S., & Hellmann, R. (2016a). Welding of transparent polymers using femtosecond laser. *Applied Physics A: Materials Science and Processing*, *122*(2), 1–4. https://doi.org/10.1007/s00339-016-9605-x

Roth, G. L., Rung, S., & Hellmann, R. (2016b). Welding of transparent polymers using femtosecond laser. *Applied Physics A: Materials Science and Processing*, *122*(2), 1–4. https://doi.org/10.1007/s00339-016-9605-x

Schricker, K., Samfaß, L., Grätzel, M., Ecke, G., & Bergmann, J. P. (2020). Bonding mechanisms in laser-assisted joining of metal-polymer composites. *Journal of Advanced Joining Processes*, *1*. https://doi.org/10.1016/j.jajp.2020.100008

Temiz, Y., Lovchik, R. D., Kaigala, G. V., & Delamarche, E. (2015). Lab-on-a-chip devices: How to close and plug the lab? In *Microelectronic Engineering* (Vol. 132, pp. 156–175). Elsevier. https://doi.org/10.1016/j.mee.2014.10.013

Tsao, C. W., & DeVoe, D. L. (2009). Bonding of thermoplastic polymer microfluidics. In *Microfluidics and Nanofluidics* (Vol. 6, Issue 1, pp. 1–16). https://doi.org/10.1007/s10404-008-0361-x

Vanwersch, P., Evens, T., Van Bael, A., & Castagne, S. (2024). Design, fabrication, and penetration assessment of polymeric hollow microneedles with different geometries. *International Journal of Advanced Manufacturing Technology*, *132*(1–2), 533–551. https://doi.org/10.1007/S00170-024-13344-X

Volpe, A., Di Niso, F., Gaudiuso, C., De Rosa, A., Vázquez, R. M., Ancona, A., Lugarà, P. M., & Osellame, R. (2015). Welding of PMMA by a femtosecond fiber laser. *Optics Express*, *23*(4), 4114. https://doi.org/10.1364/oe.23.004114

Volpe, A., Krishnan, U., Chiriacò, M. S., Primiceri, E., Ancona, A., & Ferrara, F. (2021). A Smart Procedure for the Femtosecond Laser-Based Fabrication of a Polymeric Lab-on-a-Chip for Capturing Tumor Cell. *Engineering*, *7*(10), 1434–1440. https://doi.org/10.1016/j.eng.2020.10.012

Wan, Y. J., Li, G., Yao, Y. M., Zeng, X. L., Zhu, P. L., & Sun, R. (2020). Recent advances in polymer-based electronic packaging materials. In *Composites Communications* (Vol. 19, pp. 154–167). Elsevier Ltd. https://doi.org/10.1016/j.coco.2020.03.011

Xu, J., Jiang, Q., Yang, J., Cui, J., Zhao, Y., Zheng, M., Oliveira, J. P., Zeng, Z., Pan, R., & Chen, S. (2023). A Review on Ultrafast Laser Microwelding of Transparent Materials and Transparent Material–Metals. In *Metals* (Vol. 13, Issue 5). MDPI. https://doi.org/10.3390/met13050876

Zhang, G., Bai, J., Zhao, W., Zhou, K., & Cheng, G. (2017). Interface modification based ultrashort laser microwelding between SiC and fused silica. *Optics Express*, *25*(3), 1702.

https://doi.org/10.1364/oe.25.001702